Annu. Rev. Biochem. 2005. 74:649–79
doi: 10.1146/annurev.biochem.74.082803.133130

ANTIBIOTICS TARGETING RIBOSOMES: Resistance, Selectivity, Synergism, and Cellular Regulation

Ada Yonath
Department of Structural Biology, Weizmann Institute, 76100 Rehovot, Israel; email: ada.yonath@weizmann.ac.il

Key Words ribosomal crystallography, peptide-bond formation, antibiotic synergism, nascent protein exit tunnel

■ **Abstract** Antibiotics target ribosomes at distinct locations within functionally relevant sites. They exert their inhibitory action by diverse modes, including competing with substrate binding, interfering with ribosomal dynamics, minimizing ribosomal mobility, facilitating miscoding, hampering the progression of the mRNA chain, and blocking the nascent protein exit tunnel. Although the ribosomes are highly conserved organelles, they possess subtle sequence and/or conformational variations. These enable drug selectivity, thus facilitating clinical usage. The structural implications of these differences were deciphered by comparisons of high-resolution structures of complexes of antibiotics with ribosomal particles from eubacteria resembling pathogens and from an archaeon that shares properties with eukaryotes. The various antibiotic-binding modes detected in these structures demonstrate that members of antibiotic families possessing common chemical elements with minute differences might bind to ribosomal pockets in significantly different modes, governed by their chemical properties. Similarly, the nature of seemingly identical mechanisms of drug resistance is dominated, directly or via cellular effects, by the antibiotics' chemical properties. The observed variability in antibiotic binding and inhibitory modes justifies expectations for structurally based improved properties of existing compounds as well as for the discovery of novel drug classes.

CONTENTS

INTRODUCTION

With the increased use of antibiotics to treat bacterial infections, pathogenic strains have acquired antibiotic resistance, causing a major problem in modern therapeutics. The decrease in antibiotics' effectiveness prompted extensive effort in the design of new or improved antibacterial agents. Numerous attempts have been made. Nevertheless, the results of these efforts indicate that the battle against antibiotic resistance is far from its end and further drug improvement is necessary. In addition to combating resistance, many issues should be addressed when designing new drugs or improving existing compounds, ranging from drug delivery via drug selectivity to the probable effects of drugs' metabolites.

Protein biosynthesis is one of the most fundamental processes of living cells. During the cell growth log period, the cellular components facilitating this process may account for most of the cell's dry weight. The ribosome is the universal cellular organelle translating the genetic code by catalyzing the sequential polymerization of amino acids into proteins. Being a prominent player in this vital process, many antibiotics of diverse kinds target the ribosome. Consequently, since the beginning of therapeutic administration of antibiotics, ribosomal drugs have been the subject of numerous biochemical and genetic studies [reviewed in (1–8)].

The recently determined high- and medium-resolution structures of ribosomal particles (9–13) and of their complexes with many different antibiotics (14–24) elucidated several basic concepts in antibiotic-binding modes at the molecular level, thus providing tools to assess previous findings while developing novel ideas. However, although X-ray crystallography is a powerful method for elucidating structural information of biological macromolecules, its productivity is limited by its dependence on the availability of crystals. Because ribosomes from pathogenic bacteria have not been crystallized yet, the crystallographic analyses are confined to currently available crystals. These include the small ribosomal subunit from *Thermus thermophilus*, T30S, and the large one from *Deinococcus radiodurans*, D50S (two eubacteria that resemble pathogens), as well as the large ribosomal subunit from *Haloarcula marismortui*, H50S, which shares properties with eukaryotes. The availability of crystals of large subunits from two kingdoms of life was found useful for comparative studies, which highlighted critical principles of drug selectivity. For example, the identity of nucleotide 2058 is one of the most crucial elements for binding of macrolides, an antibiotic family that acts on the large subunit. This nucleotide is an adenine in prokaryotes and guanine in eukaryotes, as well as in *H. marismortui*, and this small difference is the key for proper drug binding as well as for drug selectivity.

Concerns associated with X-ray crystallography relate to the relationship between the cellular and the crystalline structures, namely the relevance of the

crystallographic results. The similarities of the structures of wild-type T30S, as well as of its complexes with antibiotics, elucidated by two independent laboratories using two different phasing methods (9, 10, 14–16), and the ability to rationalize biochemical, functional, and genetic observations by these structures demonstrate the inherent reliability of X-ray crystallography. The consistencies of the drug locations with biochemical and resistance data, alongside the construction of the crystalline complexes at clinically relevant drug concentrations, also manifest the reliability of the crystallographic results. Consequently, it can be concluded that for complexes of ribosomes with antibiotics, dissimilarities observed crystallographically reflect genuine variability in drug-binding modes.

Indeed, the crystallographic results enabled the identification of the molecular interactions involved in antibiotic-ribosome recognition, illuminated the antibiotic-binding modes, enabled the detection of the linkage between various ribosomal functions and the antibiotics' modes of action, and led to suggestions concerning their inhibitory activity. These crystal structures also provided insight into antibiotic synergism, the complex issues of antibiotic selectivity and toxicity, and the mechanisms that pathogenic bacteria developed for acquiring resistance against antibiotics, hence putting the vast amount of available biochemical and genetic data into perspective (25–30).

Here, we discuss the structural findings associated with ribosomal antibiotic action, highlighting the unique achievements of these studies as well as their shortcomings. Covering the large amount of biochemical and medical knowledge and providing a comprehensive list of the detailed modes of action of all ribosomal antibiotics are beyond the scope of this review. Instead, we emphasize structural analysis and how it can lead to better understanding of antibiotic selectivity, synergism, and the acute problem of resistance to antibiotics.

RIBOSOMAL FEATURES TARGETED BY ANTIBIOTICS

The ribosomes are giant ribonucleoprotein assemblies, built of two subunits that assemble to produce a functional particle at the beginning of the process of protein biosynthesis. Almost all ribosome types are composed of long RNA chains, accounting for two thirds of the mass, and many different proteins. The bacterial ribosomal subunits are of molecular weights of 0.85 and 1.45 MDa. The small subunit (called 30S in prokaryotes) contains an RNA chain (16S) of ~1500 nucleotides and 20–21 proteins, and the large subunit (called 50S in prokaryotes) has two RNA chains (23S and 5S RNA) of about 3000 nucleotides in total and 31–35 proteins.

While elongation proceeds, the small subunit provides the decoding center and control translation fidelity, and the large one contains the catalytic site, called the peptidyl-transferase center (PTC), as well as the protein exit tunnel. mRNA carries the genetic code to the ribosome, and tRNA molecules bring the protein building block, the amino acids, to the ribosome. These L-shaped molecules are built mainly

of double helices, but their two functional sites, namely the anticodon loop and the 3′ end, are single strands. The ribosome possesses three tRNA-binding sites, the A (aminoacyl), the P (peptidyl), and the E (exit) sites. The tRNA anticodon loops interact with the mRNA on the small subunit, whereas the tRNA acceptor stem, together with the aminoacylated or peptidylated tRNA 3′ ends, interact with the large subunit. Hence, the tRNA molecules and intersubunit bridges, built of flexible components of both subunits, are the entities that combine the two subunits within the active ribosome (12, 33). Each elongation cycle involves decoding, the creation of a peptide bond, and the release of a deacylated tRNA molecule. It also requires the advancement of the mRNA together with the tRNA molecules from the A to the P and then to the E site, a motion driven by GTPase activity.

Ribosomal antibiotics target the decoding site, the peptidyl-transferase center, the protein exit tunnel, and several mobile elements that provide the dynamics required for protein biosynthesis, including mRNA threading and progression and nascent protein passage. They exhibit diverse modes of action. Among the antibiotic inhibitory modes studied crystallographically are miscoding [e.g., streptomycin and paromomycin (15)], minimization of ribosomal mobility [e.g., spectinomycin, hygromycin B, edeine, and pactamycin (14–16)], interference with tRNA binding at the decoding center [e.g., aminoglycosides, paromomycin, and tetracycline (15, 16)] as well as at the PTC [e.g., clindamycin, chloramphenicol, sparsomycin, streptogramin$_A$, and tiamulin (17, 20, 23, 24, 31–33)], and blockage of the protein exit tunnel [macrolides, azalides, ketolides, and streptogramins$_B$ (17–24)].

The scientific consequences of crystallographic studies on ribosomal-antibiotic complexes extend beyond the clinical or drug design aspects because they target primarily ribosomal features with functional relevance. Thus, the structural information assisted significantly the elucidation of specific ribosomal mechanisms. Examples of antibiotics that revealed novel ribosomal properties or enforced otherwise observed findings include the following: decoding (paromomycin); mRNA progression (spectinomycin and edeine); A-site binding to the small (tetracycline) and the large (chloramphenicol) subunits; PTC mobility (sparsomycin); tRNA rotatory motion (Synercid®), and tunnel gating (troleandomycin).

The Decoding Site

Decoding requires the correct codon–anticodon recognition. Analysis of the two high-resolution structures of the small subunit (Figure 1) from *T. thermophilus* (9, 10) showed that its main structural features radiate from a junction located on the intersubunit interface at the location of the decoding site. The mRNA chain wraps around the "neck" between the "head" and the "body" while progressing along an elongated curved channel, formed by the lower side of the head and the upper region of the "shoulder." A noncovalent reversible body-head connection, called "latch" (9), is the feature controlling the entrance of the mRNA into its path, which facilitates mRNA threading and provides the special geometry that guarantees processivity and ensures maximized fidelity. The most prominent feature in the decoding center is the upper portion of helix H44 (*Escherichia coli* nomenclature

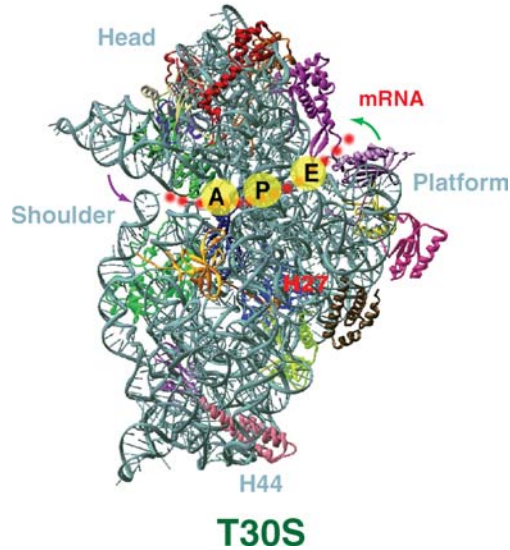

Figure 1 The crystal structure of the small ribosomal subunit from *Thermus thermophilus*, T30S (9), seen form the interface side. Ribosomal RNA is shown in gray. The main chains of the various proteins are shown as ribbons, colored arbitrarily. Selected functional relevant features are shown with their traditional names. The approximate positions of the tRNA anticodon loops of the A-, P- and E-site tRNA are marked. The approximate mRNA path is shown by red dots. The arrows designate the suggested head and platform motions involved in mRNA translocation. Among them, the purple arrow symbolizes the head motion required for the formation of the mRNA entrance pore, and the green arrow shows the correlated platform motion, enabling mRNA progression. H44 shows the bottom end of helix 44, which stretches all the way to the decoding site (P). H27 designates the switch helix, which provides the tetracycline secondary binding site. A-site tRNA is the primary binding site of tetracycline, and E is located in the vicinity of edeine binding.

system is being used throughout). This helix (Figure 1) extends from the decoding site toward the other end of the subunit. It is located midway between the two sides of the subunit, on the rather flat intersubunit interfaces, and forms most of the intersubunit contacts in the assembled ribosome. An additional important feature in the decoding region is helix 27, H27, called the switch helix, that can undergo alterations in its base-pairing scheme, which may trigger global conformational rearrangements essential to mRNA translocation (34).

Among the structurally analyzed antibiotics that target the small subunit, some aminoglycoside drugs (14–16, 35–38) as well as tetracycline (15, 16) block tRNA-binding sites at the decoding center. Other antibiotics are involved in the dynamics of translocation and tRNA selection. For example, hygromycin B restricts the movement of helix H44 and, hence, limits or inhibits the conformational changes

crucial for the movement of this helix during translocation, and the antibiotic confiscates the tRNA in the A site (15). Pactamycin and edeine seem to intervene with mRNA progression by blocking its path or by freezing the dynamics of the platform (Figure 1) associated with this motion (15, 16). Spectinomycin inhibits elongation-factor-G-catalyzed translocation of the peptidyl-tRNA from the A site to the P site by binding near the pivot point of the head movement. Streptomycin, however, stabilizes the state that has a higher tRNA affinity (14), and a secondary binding site of tetracycline was proposed to hinder the motions of the switch helix H27 (Figure 1), suggested to facilitate mRNA progression (34).

Similar to streptomycin, the aminoglycoside paromomycin increases the error rate of translation. Analysis of its modes of binding within the small subunit (14), as well as the comparisons to its interactions with model RNA fragments (35–38), provided insights into the decoding mechanism, highlighting the importance of the conformations of nucleotides A1492 and A1493 in the selection of cognate tRNAs.

The Ribosomal Catalytic Site

Analysis of the structures of functional complexes of D50S revealed that the ribosome provides the frame for right substrate positioning for peptide bond formation and amino acid polymerization (31, 32, 39–41) and that the peptide bond is being formed within a universally sizable symmetrical region. This region is located in and around the PTC, within domain V of the 23S RNA (Figure 2), and connects various ribosomal functional elements, including the tRNA entrance and exit regions as well as the feature bridging the PTC with the decoding site (Figure 3).

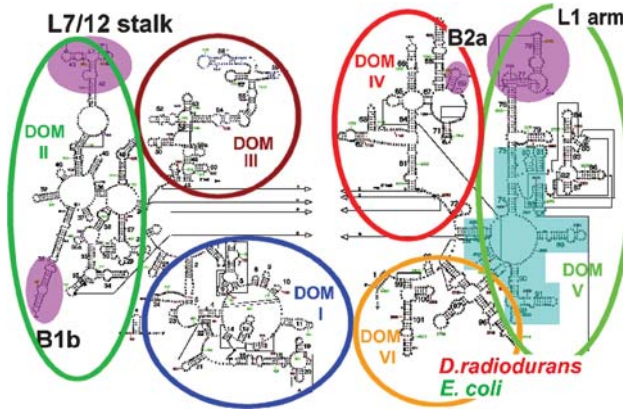

Figure 2 The two-dimensional diagram of the 23S RNA from *Deinococcus radiodurans* (13) and *E. coli.* The different RNA domains are encircled. The area highlighted in cyan is the symmetry-related region. The regions shaded in dark pink are highly flexible and, hence, readily become disordered, as observed in the large subunits from *Haloarcula marismortui*, H50S (11).

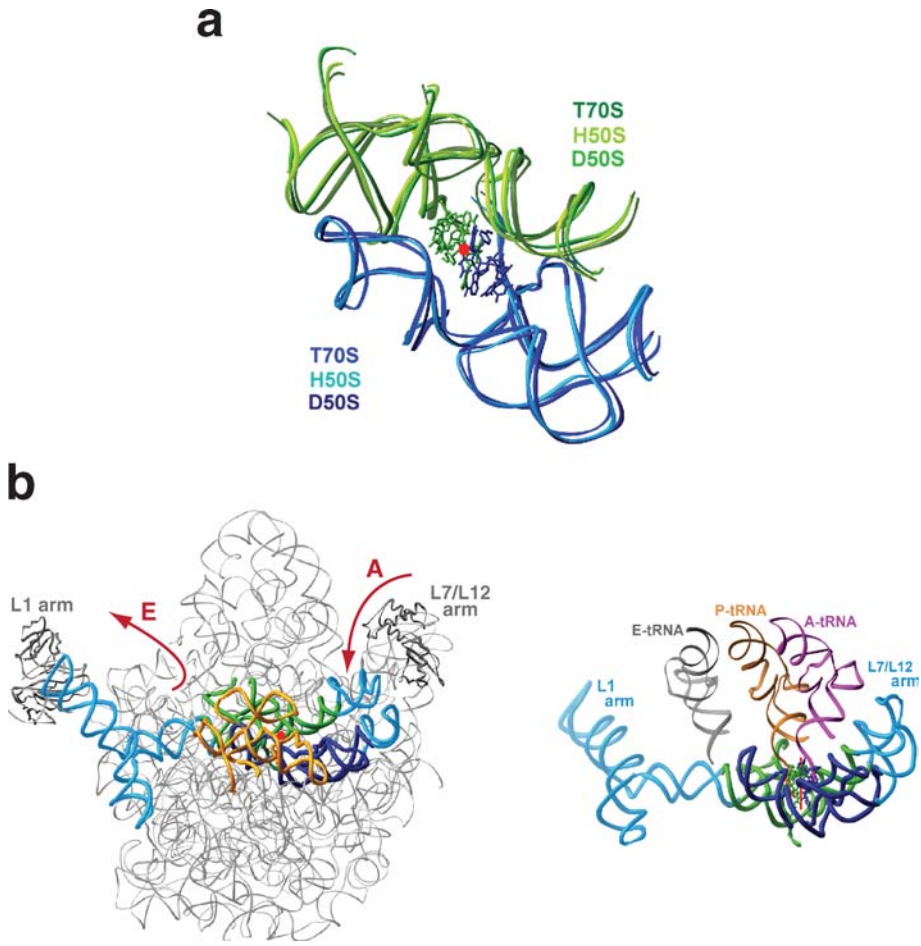

Figure 3 (*a*) Superposition of the backbone of the symmetrical regions in all known ribosome structures: the entire ribosome form from *T. thermophilus*, T70S (12); H50S (11); and the large subunits from *D. radiodurans*, D50S (13). The green colors designate the region containing the P loop, and the blue colors contain the A loop. The red dot is the location of the twofold axis of the symmetry-related region. Note a substrate analog in the A site (*blue*) (31) and its derived P site (*green*). (*b*) (*left*) The location of the symmetry-related region within in the large ribosomal subunit of D50S (represented by the backbones of its 23S and 5S RNA chains, shown as *gray ribbons*). Three of its nonsymmetrical extensions (*cyan*) and the twofold symmetry axis (*red*) are also shown. The red arrows indicate the approximate directions of the incoming A-site and E-site tRNA (A and E, respectively). The gold ribbon is the intersubunit bridge (B2a) that combines the two ribosomal active sites. (*right*) The top view, but without the ribosomal RNA, and with the twofold axis, as well as the A-site substrate analog and its derived P-site mate. The positions of the three tRNA were obtained by docking the structure of the T70S complex onto D50S (12).

A universal base pair, formed between a ribosomal A-site donor (G2553) and C75 of the tRNA CCA end, contributes to the overall positioning of the aminoacylated A-site tRNA, whereas remote interactions position this tRNA molecule at its accurate orientations within the PTC (31, 32, 39–41). At this orientation, the bond connecting the tRNA single-stranded 3′ end with the rest of the tRNA molecule almost coincides with the ribosomal symmetry axis. This implies that the A- to P-site passage is a combination of two types of motion, reformed in conjunction: the sideways mRNA/tRNA translocation that applies to the A-site tRNA molecule except for its 3′ end and the rotatory motion of the aminoacylated tRNA end within the PTC (Figure 4).

The rotatory motion is navigated and guided by the striking architectural design of the PTC (Figure 4) and terminates in stereochemistry appropriate to the nucleophilic attack of the A-site amino acid on the carbonyl carbon of the peptidyl tRNA at the P site (31, 32, 39–42). Flexible elements of the PTC, namely the two universally conserved nucleotides A2602 and U2585, bulge out toward the PTC center (Figure 4) and do not obey the symmetry. Their crucial contributions to anchoring and propelling the rotatory motion (31, 32, 39–41) and consequently to peptide bond formation are demonstrated by their universality and by the roles that they play as targets for antibiotics (see below, in Ribosomal Dynamics and Antibiotic Synergism).

Structurally, the antibiotics that target the PTC can be divided into two groups. The members of the first group block substrate binding or interfere with the formation of the peptide bond. The members of the second group hinder the PTC or the substrate motions. Blockage of substrate binding is the simplest mode of antibiotic action. It requires a high drug affinity to the target, which may be achieved by optimized stereochemistry binding. Chloramphenicol, clindamycin, tiamulin, sparsomycin, and streptogramin$_A$ target the PTC (Figure 5) (17, 23, 24, 31), and despite the limited space and the apparently similar outcome of their binding, each of these compounds acts in a different way. Chloramphenicol blocks only the A site, whereas clindamycin, tiamulin, and streptogramin$_A$ bind to both the A and the P sites. Also, marked differences have been observed in the interplay between their binding and the conformation of their targets. Whereas chloramphenicol and clindamycin cause hardly any conformational modifications, tiamulin induces subtle changes, and sparsomycin (31) and streptogramin$_A$ (23) act by triggering substantial alterations.

Chloramphenicol, the first antibiotic of the large ribosomal subunit investigated crystallographically (17), hampers protein biosynthesis by occupying the PTC A site (Figure 5), which is consistent with most of the biochemical and resistance data (43–45). Clindamycin, an antibiotic agent belonging to the Lincosamides family, is another example of a PTC-binding drug (46). In D50S, it connects between the PTC and the ribosome exit tunnel (Figure 5), thus reducing the level of ribosomal flexibility in this area (17). This unique binding mode should be extremely efficient and is consistent with its increased potency in treating infections caused by anaerobic bacteria or by *Toxoplasma gondie* or *Pneumocystis carinii* in individuals

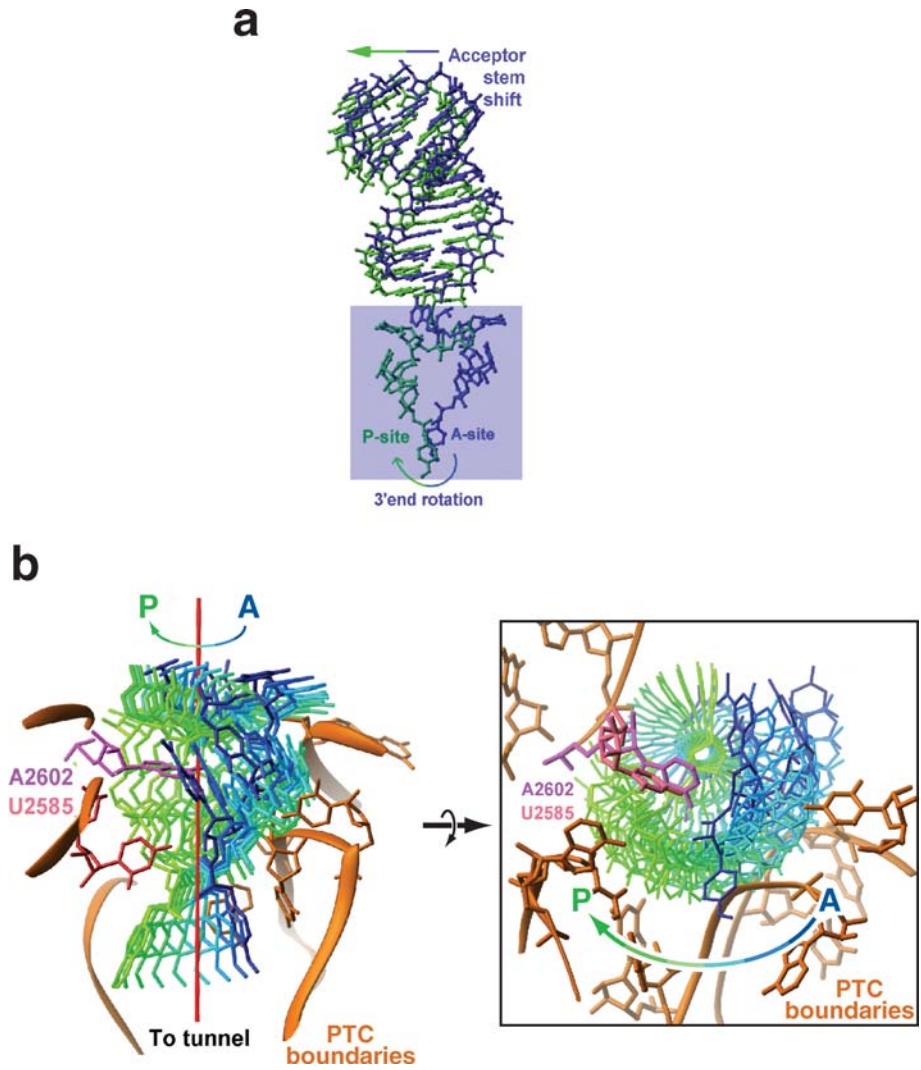

Figure 4 (*a*) Translocation by the rotatory mechanism. The shaded area, namely the single-stranded tRNA 3′ end, passes from A to P by rotation around the bond connecting it to the helical part of the tRNA, which translocates by a shift. (*b*) Two orthogonal views of snapshots of the spiral rotatory motion, obtained by successive spiral rotations (15° each) of the tRNA 3′ end around the twofold axis, from the A to the P site. Note that both tRNAs' ends point into the exit tunnel. The ribosomal components, belonging to the PTC rear wall, that confine the exact path of the rotatory motion are shown in gold, and the two front wall flexible nucleotides, A2602 and U2585, are colored in magenta and pink, respectively. The A-P passage is represented by the transition from the A-site aminoacylated tRNA (in *blue*) to the P site (in *green*). The blue-green rounded arrows show the rotation direction. A view from the tunnel into the PTC.

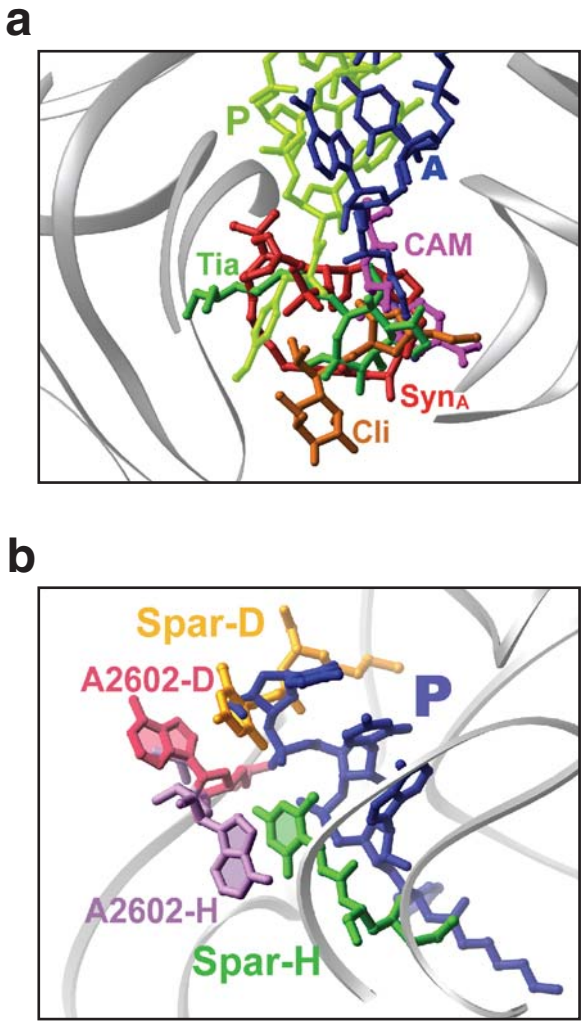

Figure 5 (*a*) PTC antibiotics together with the 3′ ends of the A- and the P-site substrates in D50S. The backbone of the PTC wall is represented by gray ribbons. The abbreviations are CAM, chloramphenicol; Cli, clindamycin; Tia, tiamulin; and Syn_A, the $streptogramin_A$ component of Synercid®. (*b*) Sparsomycin-binding sites in D50S (Spar-D) and H50S (Spar-H), manifesting the marked difference in binding modes that originate from the ribosomal functional state because it was bound by itself to D50S and together with a P-site mimic to H50S. The P-site substrate analog position, as seen in the structure of its complex with H50S and sparsomycin, explains why sparsomycin may stabilize nonproductive P-site tRNA binding. Note that the bases involved in stacking interactions (between sparsomycin and A2602 in its two positions) are filled.

with AIDS, as well as for management of malaria resulting from *Plasmodium falciparum* resistant strains (47).

The pleuromutilin antibiotic family is among the antibiotics that are currently being subjected to intensive improvement efforts (48, 49). Tiamulin, which belongs to the pleuromutilin class of antibiotics (50), inhibits peptide bond formation (51–53). It binds to the PTC of D50S with its tricyclic mutilin core positioned in a tight pocket at the A-tRNA-binding site, and the extension protruding from it partially overlaps with the P-tRNA-binding site. Hence, tiamulin can be considered both as an A-site and as a P-site blocker. This binding mode is consistent with tiamulin-resistant mutants in *Brachyspira* sp. isolates (54) as well as with known competition between tiamulin and chloramphenicol, puromycin (55), and carbomycin A (53).

The Nascent Protein Exit Tunnel and Its Inhibitors

Nascent proteins emerge out of the ribosome through an exit tunnel, as first seen in the mid-1980s (56, 57). This tunnel is located below the PTC and spans the large subunit (Figure 6). It is lined primarily by ribosomal RNA, but several ribosomal proteins reach its wall. Two of them, namely proteins L4 and L22, create an internal constriction. Four years ago, when first observed at high resolution in H50S crystal structure, this tunnel was assumed to be a passive and inert conduit for nascent chains (11, 58). However, recent biochemical findings show that the ribosomal exit tunnel is a dynamic functional entity with the ability to take part in elongation discrimination, arrest, and perhaps partial protein folding (59–61), and antibiotic research enabled the detection of its dynamic properties that may be required for its involvement in cellular regulation.

TYPICAL MACROLIDES The nascent protein exit tunnel possesses a pocket of a high affinity for antibiotics of the macrolide, ketolide, and streptogramin$_B$ families. This pocket is located at the upper side of the tunnel, below the PTC and above the tunnel constriction (Figure 6). Macrolides and ketolides, which rank highest in clinical usage, bind to this high-affinity pocket either in vacant or to translating ribosomes, carrying a very short nascent peptide (62–65). By binding, the useful antibiotics block nascent proteins' progression through the exit tunnel, which, in turn, causes an arrest of elongation (17–23, 65–67). This arrest leads to dissociation of short peptidyl-tRNAs from the ribosome, explaining why the macrolides were originally thought to interact with the PTC (65, 68, 69).

The macrolide-ketolide antibiotic family consists of natural or semisynthetic compounds with a lactone ring to which one or two sugars are attached. The first widely used macrolide drug was erythromycin, a 14-member lactone ring, decorated by a desosamine and cladinose sugars. All currently available crystal structures of 14-membered-ring macrolide complexes with large subunits (17, 21) show that the interactions of the binding pocket components with the desosamine sugar and the lactone ring play a key role in macrolide binding. These contacts involve predominantly the main constituents of the macrolide-binding pocket,

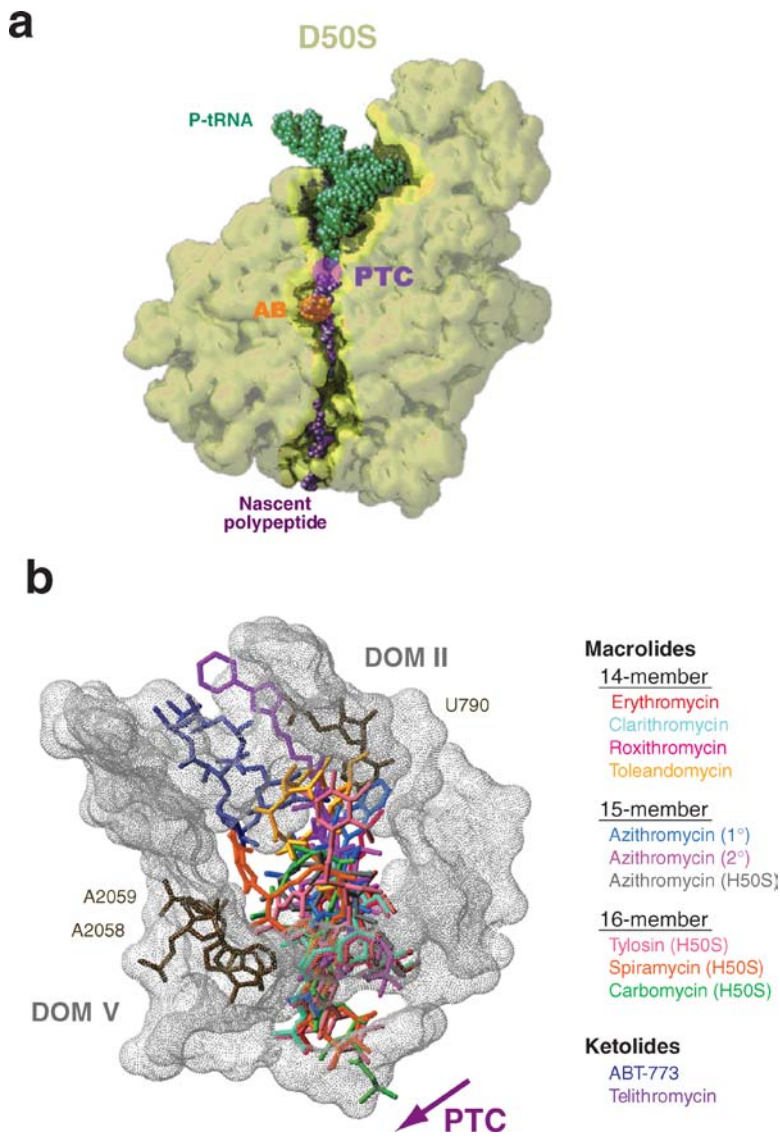

Figure 6 (*a*) A section of the ribosomal large subunit (D50S), which highlights the ribosomal tunnel and shows the approximate location of the PTC and the macrolide antibiotics. (*b*) The binding modes of several antibiotics within a cross section of the ribosomal tunnel of D50S (*dotted gray cloud*) at the level of the macrolide-binding pocket. The positions of the key nucleotides for macrolide-ketolide binding, selectivity, and resistance in domains V (DOM V) and II (DOM II) are marked. For orientation, the direction of the peptidyl-transferase center (PTC) is marked. The binding modes of 15- and 16-membered-macrolactone ring compounds H50S are also shown. Another abbreviation is ABT-773 (also called cethromycin).

namely nucleotides A2058–A2059 of the 23S RNA domain V (Figures 2 and 6). The second macrolide sugar, namely the cladinose, interacts directly with the ribosome in only a few cases (21).

Three closely related 14-membered macrolides, erythromycin and its semisynthetic derivatives, clarithromycin and roxithromycin, exhibit exceptional consistency in their binding modes to the macrolide-binding pocket (Figure 7) (17). Their high binding affinities originate mainly from hydrophobic interactions of their lactone rings and hydrogen bonds of their desosamine sugars with nucleotides A2058 and A2059. Erythromycin binding mode indicates that nucleotide 2058 plays a key role in macrolide binding and selectivity as it is an adenine in eubacteria and a guanine in eukaryotes (for more detail, see below in Adenine Versus Guanine). Furthermore, the prominent macrolides-lincosamides-streptogramin$_B$ (MLS) resistance mechanisms, A to G substitution or *erm*-gene methylation, are based on increasing the size of A2058 (1–3, 28, 70–72). Because erythromycin, clarithromycin, and roxithromycin were the first macrolides to be studied crystallographically, the similarity of their binding modes raised expectations for comparable resemblance in the binding modes of all macrolides (30). By analogy, similar resistant mechanisms were anticipated for all macrolides, an assumption that was shown later to be oversimplified (42).

MACROLIDE DERIVATIVES To circumvent the acute problems associated with macrolide resistance, several new compounds have been designed. These include macrolide derivatives in which the core macrolactone ring has a higher flexibility by increasing the number of its atoms, similar to the 15-member ring azithromycin as well as 16-member ring derivatives, such as tylosin, carbomycin A, spiramycin, and josamycin [which exhibit activity against some MLS resistance strains (73–75)]. Ketolides present yet another chemical approach based on the addition of rather long extensions, such as alkyl-aryl or quinollyallyl, to the core macrolactone ring; this approach is expected to provide additional interactions, thus minimizing the contribution of 2058–2059 region. The macrolactone ring of the ketolide is characterized by the presence of a keto group instead of the cladinose sugar at its C3 position, an 11,12-cyclic carbamate (76–83).

Recent structural studies showed that the expectations of a uniform binding mode and resistance mechanism were not fulfilled, even within members of closely related antibiotic families (29), such as the macrolide-ketolide group. Thus, it was shown that although all macrolides exploit the same high-affinity pocket, their conformations, orientations, and specific interactions might vary in accordance with their chemical nature (Figures 6 and 7). Yet, the basic nature of the macrolides' and ketolides' inhibitory action is similar, namely to hamper protein biosynthesis by blocking the protein exit tunnel.

Consistent with biochemical results (84, 85), the crystal structures of complexes of the large ribosomal subunit with the 15- and 16-membered-ring macrolide (18, 19), as well as with ketolide (18, 22), revealed drug interactions with domain II in addition to the common macrolide interactions with domain V (Figures 2 and 6).

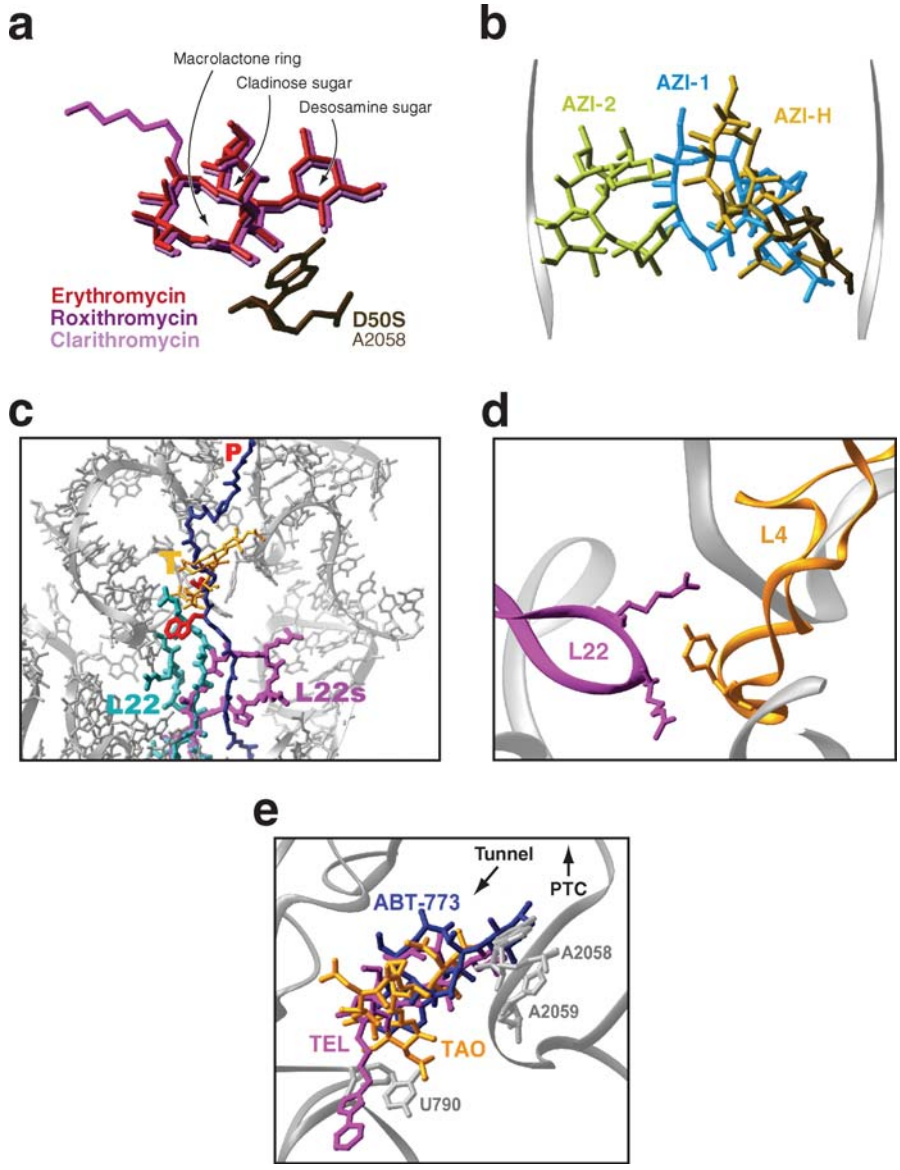
a
Macrolactone ring
Cladinose sugar
Desosamine sugar
Erythromycin
Roxithromycin
Clarithromycin
D50S
A2058
b
AZI-1
AZI-2
AZI-H
c
P
T
L22
L22s
d
L4
L22
e
Tunnel
PTC
ABT-773
A2058
A2059
TEL
TAO
U790

Domain II lines the tunnel wall approximately across domain V and is likely to provide additional drug interactions that may compensate for the loss of the seemingly vital contacts of the desosamine sugar with A2058 in MLS-resistant strains.

The addition of a nitrogen atom to the 14-membered macrolide to produce the 15-membered macrolide, azithromycin, increases the flexibility of the lactone ring, alters its conformation, and induces novel interactions. Three distinctly different orientations have been observed for the bound azithromycin (18, 19), each of which differs from that of erythromycin (17) and supports this suggestion. Within D50S, azithromycin binds cooperatively at two sites, which interact with each other. Both azithromycin molecules bind perpendicular to the tunnel direction, stretching from the typical erythromycin pocket to domain II. Consequently, azithromycin occupies most of the tunnel free space (Figure 7), which is consistent with its high efficiency and prolonged action (76). The unusual dual binding of azithromycin to D50S may be species specific because it involves contacts with a nonconserved glycine 60 of protein L4 (18, 27). However, these contacts are with the backbone of this protein, and the direction of its side chain points away from the interaction

←

Figure 7 (*a*) The chemical composition and the common binding mode of erythromycin, clarithromycin, and roxithromycin in the protein exit tunnel of D50S. The main macrolide components, namely the macrolactone ring and the desosamine and cladinose sugars, are marked. (*b*) Superposition of azithromycin bound to H50S (AZI-H) and to D50S (AZI-1 and AZI-2), together with the position of A2058 and the approximate boundary of the ribosome tunnel (*gray ribbons*). (AZI-1 and AZI-2 are the primary and secondary sites of azithromycin in D50S.) Note that according to this view, azithromycin binding to H50S should not severely hamper nascent protein passage, which explains drug selectivity. (*c*) A view into the tunnel (*gray*), showing the troleandomycin (T, in *gold*)-induced swinging (*magenta*) of protein L22 beta-hairpin tip (native orientation shown in *cyan*). The modeled polypeptide chain (*purple*) represents a nascent protein with the sequence motif known to cause SecM (secretion monitor) elongation arrest. This motif is located about 150 residues from the N terminus and has the sequence XXXXXWXXXXXXXXXP, where X is any amino acid and P (proline) is the last amino acid to be incorporated into the nascent chain (59). The position of the tryptophane essential for elongation arrest is also shown to indicate the stunning correlation between it and that of troleandomycin. The SecM proline required for the arrest when incorporated into the protein is the top amino acid of the modeled nascent chain, located at the PTC, at the end of the P-site tRNA. (*d*) A possible interaction between protein L22 beta-hairpin tip in its swung conformation and Tyr 59 of protein L4, which forms (together with L22) the tunnel constriction. (*e*) Superposition of the locations of troleandomycin (TAO) and the two ketolides: cethromycin (ABT-773) and telithromycin (TEL). Key nucleotides for ketolide binding from domain V and II are shown. Tunnel walls are represented by a gray ribbon. For orientation, the PTC direction is indicated.

region. Hence, the identity of the residue at position 60 of protein L4 position is of marginal relevance for L4 ineractions with the second azithromycin molecule. In addition, modeling and energetic considerations indicated the feasibility of dual azithromycin binding to ribosomes of several pathogens, such as *Haemophilus influenzae*, *Mycobacterium tuberculosis*, *Helicobacter pylori*, *Mycoplasma pneumoniae*, and *Mycobacterium leprae* (32). Furthermore, isolates of the azithromycin resistant strain of *Streptococcus pyogenes* were characterized as having deletions in the vicinity of residue 60 of protein L4 of the pathogen (86), therefore indicating possible azithromycin interactions with protein L4 and supporting azithromycin dual binding. Because L4 is located deeper in the tunnel compared to the macrolide-binding pocket (13), the involvement of L4 in azithromycin resistance further supports the crystallographic results showing azithromycin interactions with this region and questions the validity of counterclaims obtained by combining results of mutagenesis of A2058 and A2059 and of the assumption that 15-membered-ring macrolides bind to the ribosome identically to the 14-membered ring (30).

TROLEANDOMYCIN: A MACROLIDE INTERACTS WITH TWO DOMAINS AND TRIGGERS TUNNEL GATING Troleandomycin is a 14-membered-ring macrolide in which all hydroxyl groups are either methylated or acetylated; for this reason, it cannot create the typical macrolide hydrogen bonds. The lack of hydroxyls available for hydrogen bonds and the larger size of troleandomycin compared to that of erythromycin dictate a unique binding mode, although in the crystals of its complex with D50S troleandomycin binds to the typical macrolide 2058–2059 pocket (21). The utilization of a unique set of interactions demonstrates that functionally meaningful interactions of macrolides with A2058 can involve various chemical moieties. Owing to the bulkiness of its substituents and its larger size, a troleandomycin lactone ring is oriented with a small inclination to the tunnel wall, rather than perpendicular to it. In its unique orientation, troleandomycin reaches from domain V to domain II and appears to collide with the tip of the beta-hairpin of protein L22. This collision seems to trigger a swing of the beta-hairpin tip across the tunnel (Figure 7) (21). Both the native and the swung conformations of L22 beta-hairpin are stabilized by electrostatic interactions and hydrogen bonds with RNA segments of the tunnel wall. Furthermore, the swung L22 beta-hairpin tip reaches the vicinity of the tunnel constriction and may interact with protein L4 (Figure 7). This L4-L22 proximity may be linked to macrolide resistant mechanisms involving mutations of these two proteins, despite the lack of direct interactions with them. In its swung conformation, the L22 beta-hairpin tip gates the tunnel, and its interactions with domain II nucleotides are correlated with mutations bypassing tunnel arrest (59), hence providing the structural basis for conformational dynamics of the tunnel and validating evidence of the tunnel discrimination properties, obtained biochemically (59–61). Protein L22 is an elongated ribosomal protein that stretches along the large subunit between the tunnel constriction and a location close to the tunnel

opening. Thus, it may participate in tunnel arrest as well as in signal transmission associated with the nascent protein progression, between the cell and the ribosomal interior.

Interestingly, troleandomycin's main interactions with domain II of D50S are through the same nucleotide, U790 (21), that interacts with each of the two ketolides, telithromycin and cethromycin, also called ABT-773 (Figure 7) (18, 22), despite the significant differences in the binding modes of these three antibiotics. This specific interaction may be responsible for troleandomycin-ketolide cross-resistance mutation and for the similarity in RNA probing (D. Baram, T. Auerbach, and I. Greenberg, unpublished results). An additional common motif between troleandomycin and ketolides is the nature of peptides mediating resistance to them. These resistant peptides (65, 87) are usually quite short (built of a few amino acids) and may displace part of the macrolide molecules in bacterial cells, thus increasing the fraction of drug-free ribosomes and consequently rendering cells resistant to macrolides (88–90).

The structures of ribosome-antibiotic complexes explain the relationship between the size of the lactone ring substituents and the number of residues that can be incorporated into nascent polypeptides by ribosomes treated with macrolides. The correlation observed between the space available for nascent peptides in the tunnel of drug-bound ribosomes and the length of peptides bound to peptidyl-tRNAs that dissociate from ribosomes upon macrolide binding (65) provides an additional support for the crystallographic position of troleandomycin. An example is carbomycin A, a 16-membered macrolide that carries a large mycaminose-mycarose sugar moiety. When bound to a *H. marismortui* ribosome (19), this extension reaches the peptidyl-transferase center, a finding correlating well with dissociation of peptidyl-tRNAs containing 2–4 residues (19, 65, 75, 91). In contrast, erythromycin, which binds to the macrolide pocket but does not possess a mycaminose-mycarose sugar, causes dissociation of peptidyl-tRNAs containing 6–8 residues (65). Telithromycin induces the release of peptidyl-tRNAs containing 9–10 residues, which is consistent with its position deeper in the tunnel, compared to typical macrolides (21).

The accumulated information concerning the modes of binding and the actions of the macrolide derivatives provides tools for addressing the important issue of the influence of the antibiotic chemical properties, conformational flexibility of their binding modes, and resistant mechanisms. For example, both troleandomycin and the ketolides are 14-membered macrolides, both bind at the 2058–2059 pocket, both interact with domain II, both have the same minimum inhibitory concentration values (for *D. radiodurans*), and both were shown to induce a similar resistant mutant (T. Auerbach, D. Baram, and I. Shalit, unpublished results). Nevertheless, the ketolides and troleandomycin exhibit significantly different binding patterns (Figure 7), resulting from their specific chemical and geometrical properties. It appears, therefore, that binding to a specific pocket or that comparable properties of different antibiotics may or may not result from comparable drug orientations.

Similarly, resistance could originate from disruption of various interactions. Therefore a specific mutation acquiring resistance to several antibiotics does not necessarily show that all have the same binding mode.

Ribosomal Dynamics and Antibiotic Synergism

The two universally conserved nucleotides, A2602 and U2585, which are of utmost importance for peptide bond formation, are favorable ribosomal targets (23, 31, 32). Both bulge out toward the center of the PTC and play crucial roles in peptide bond formation by facilitating and anchoring the rotatory motion, respectively (31, 40, 41). Interestingly, significant conformational changes are associated with the binding of antibiotics to these nucleotides, presumably because of the unusual flexibility of these nucleotides (31, 32). Indeed, even the mere binding of tiamulin and dalfopristin (92) (the streptogramin$_A$ antibiotic component of Synercid®), both of which block the PTC rather than interfering with its mobility, induces some shifts in the positioning of these two nucleotides (24). This finding is consistent with their altered chemical reactivity in the presence of these drugs (53).

Sparsomycin, which targets A2602 (20, 31, 93), is a potent universal antibiotic agent, hence less useful as an anti-infective drug. Comparisons between the two observed sparsomycin-binding sites indicated a significant correlation between the mode of antibiotic binding and the ribosomal functional state. Thus, by binding to nonoccupied large ribosomal subunits, sparsomycin stacks to the most flexible nucleotide A2602 and causes striking conformational alterations in the entire PTC. These, in turn, should influence the positioning of the tRNA in the A site, thus explaining why sparsomycin was considered to be an A-site inhibitor, although is does not interfere with A-site substrates (93–95). In its position in D50S, sparsomycin faces the P site (Figure 5) and can enhance nonproductive tRNA binding (95). Conversely, when sparsomycin enters the large subunit simultaneously with a P-site substrate or substrate analog, it can cause only a modest conformational alteration of A2602, and because the P site is occupied by the P-site substrate, sparsomycin stacking to A2602 appears to face the A site (Figure 5) (20).

In contrast to the universality of sparsomycin, Synercid® interacts partially with nonconserved nucleotides, thus exhibiting a high level of selectivity against bacterial pathogens (23, 32). This recently approved injectable drug, with excellent synergistic activity, is a member of the streptogramin antimicrobial drug family in which each drug consists of two synergistic components (S_A and S_B), capable of cooperatively converting weak bacteriostatic effects into lethal bactericidal activity. In crystals of the D50S-Synercid® complex, obtained at clinically relevant concentrations, the S_A component, dalfopristin, binds to the PTC in a manner overlapping almost perfectly the tiamulin location. However, contrary to tiamulin, which causes a modest conformational alteration of U2585, dalfopristin induces remarkable conformational alterations, including a flip of 180° of U2585 base (Figure 8), hence paralyzing its ability to anchor the rotatory motion and to direct the nascent protein into the exit tunnel (32). As this motion is of utmost importance to cell vitality, it is likely that the pressure to maintain the processivity of protein

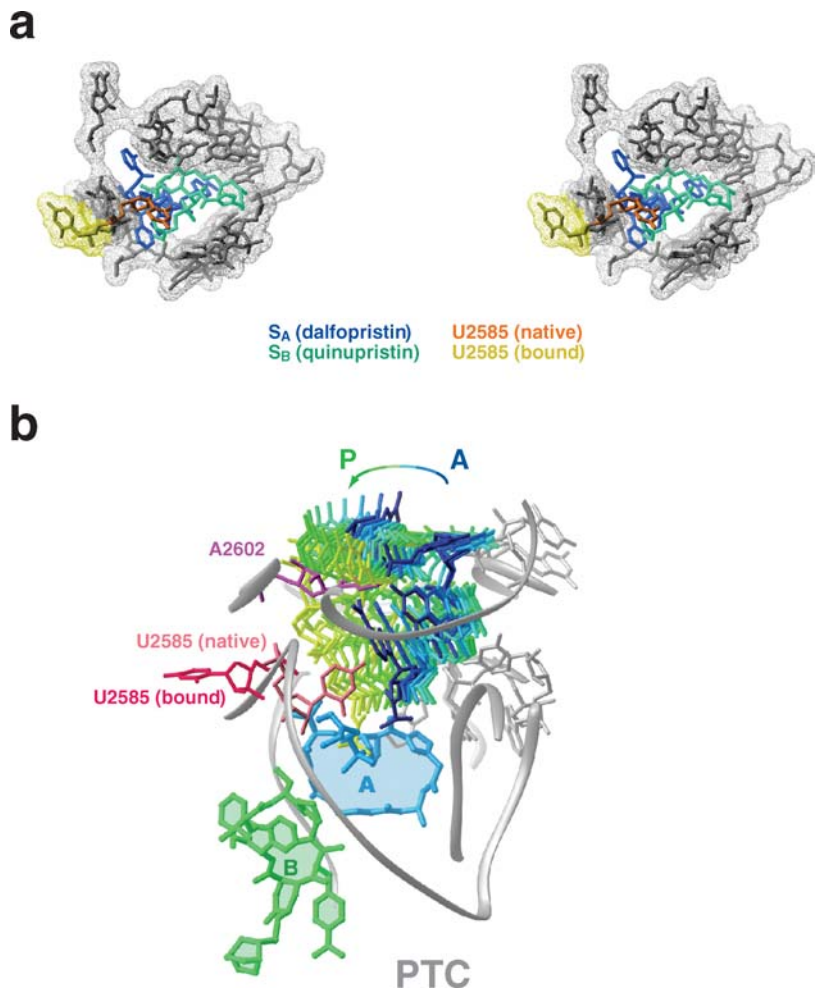

Figure 8 (*a*,*b*) Two views of the region containing the PTC and the tunnel entrance, perpendicular and parallel to the tunnel long axis, respectively, showing the synergistic action of Synercid®. Note the spectacular flip of U2585 from its native orientation to the drug bound. The relatively large height difference between the two components is clearly shown in (*b*). The positions of S_A (A), namely dalfopristin, and S_B (B), namely quinupristin, the two components of Synercid® compounds along the tunnel, can be estimated from the stereo pair shown in *(a)* and the view shown in *(b)*.

biosynthesis will attempt recovery of the correct positioning of U2585 by expelling or relocating dalfopristin, which is consistent with dalfopristin's poor antibacterial effects. The S_B component of Synercid®, quinupristin, is a macrolide that binds to the common macrolide-binding pocket (17, 29). However, owing to its bulkiness, quinupristin is slightly inclined within the tunnel and, consequently, does not block

it efficiently (23, 32), thus rationalizing its reduced antibacterial effects compared to erythromycin. When bound simultaneously, both Synercid® components interact with each other, stabilizing the nonproductive flipped positioning of U2585 and blocking the way out of dalfopristin (Figure 8). Therefore, the antimicrobial activity of Synercid® is greatly enhanced.

Thus, the two components of this synergetic drug act in two radically different fashions. Quinupristin, the S_B component, takes a passive role in blocking the tunnel, whereas dalfopristin, the S_A component, plays a more dynamic role by hindering the motion of a vital nucleotide at the active site, U2585. It is conceivable that such mode of action consumes higher amounts of material compared to the static tunnel blockage. This explanation is consistent with the peculiar composition of 70% dalfopristin and 30% quinupristin in the optimized commercial Synercid, although the crystal structure of the complex D50S-Synercid indicates binding of stoichiometric amounts of both components to each ribosomal subunit. Contrary to the potency of Synercid® action on eubacteria, streptogramins have marginal inhibitory effect on eukaryotes. Although streptogramins can bind to some archaeal species, such as archaeon *Halobacterium halobium* (92), crystals of H50S soaked in solution containing both streptogramins were found to contain only the streptogramin$_B$ component (19). Furthermore, virginiamycin-M, a streptogramin S_A component, that binds to H50S causes only minor alterations in the conformation of U2585 (19), contrary to the 180° flip of U2585 in D50S (23), and thus hardly influences the A-site to P-site rotatory motion. This very different binding mode is likely to result from the conformation of the PTC of the archaeal H50S, which varies significantly from that of the typical eubacterial ribosome (12, 13, 33). It is also consistent with the inability of the PTC of H50S to bind the peptide bond formation blocker, clindamycin, and the A-site tRNA competitor (43–45), chloramphenicol (20).

ANTIBIOTIC SELECTIVITY: THE KEY FOR EFFECTIVE THERAPEUTIC TREATMENT

Drug selectivity is the key for therapeutical effectiveness. Universal drugs, such as sparsomycin, are essentially useless for combating infections but may be used in antitumor treatment. Edeine is the example of ultimate potent universality, as its usage may be fatal. Even lower degrees of selectivity may cause toxicity. In the case of ribosomal antibiotics, which show a high level of universality in sequence and almost complete identity in function, this imperative distinction is achieved by subtle structural differences within the antibiotic-binding pockets of the prokaryotic and eukaryotic ribosomes (8, 29). The availability of structures of antibiotics complexed with the large ribosomal subunit from the eubacterium *D. radiodurans*, D50S (17, 18, 21–24), alongside the archaeon *H. marismortui*, H50S (19, 20), which possesses typical eukaryotic elements at the principal antibiotic targets, provides unique tools for investigating selectivity principles.

Adenine Versus Guanine

The structural differences determining drug selectivity may boil down to the identity of a single nucleotide. A striking example is the immense influence of the minute difference between adenine and guanine, which was found to dictate the preference of binding as well as the level of activity. Two examples are the effect of paromomycin on the small ribosomal subunit and of the typical macrolides on the large one. The interactions between paromomycin and bases A1408 and G1491 of the A site of bacterial rRNA include hydrogen bonds (with A1408) and ring stacking against G1491 (14). In humans, the identities of the homologous bases are G and A, thus hampering the creation of efficient drug-target interactions.

Similarly, the identity of the nucleotide at position 2058, the main component of the macrolide-binding pocket, governs typical macrolide selectivity. In all eubacteria, this nucleotide is an adenine that provides the means for the prominent macrolide interactions. In eukaryotes, as well as in the archaeon *H. marismortui*, it is a guanine. Structural analysis of the complexes of the typical macrolide show that guanine in this position should be too bulky to allow interactions with typical 14-membered-ring macrolides. This interpretation appears to be in accord with the resistance mechanisms (mentioned above) acquired by the increase of the space consumed by this nucleotide either by mutagenesis or by *erm* methylation.

Significant variability was observed in binding modes and binding conditions of azithromycin, a 15-membered-ring macrolide designed to overcome macrolide resistance. As with other antibiotics, azithromycin binding to H50S requires extremely high drug concentrations (19), and instead of practically blocking the D50S tunnel, in H50S azithromycin occupies only a small part of it. Thus, although it interacts with the macrolide pocket, its lactone ring is inclined, and its orientation seems to permit nascent protein progression (Figure 7). Careful analysis of the azithromycin-binding mode to H50S indicated that its peculiar mode of interaction is due not only to the existence of G in position 2058, but also to the conformation of the entire binding pocket. Hence the types and the orientations of several nucleotides within the binding site pocket are significantly different from their orientations and types in eubacterial ribosomes (42) (Figure 9).

Common to the binding modes of the 15-membered-ring azithromycin and the three 16-membered macrolides, tylosin, carbomycin, and spiramycin to H50S (19), which contains a guanine in position 2058, are their locations within the tunnel and their inclination to the tunnel wall. Comparison of the binding modes of the 16-membered-ring macrolides to H50S (19) with those of the erythromycin family to D50S (17) showed that, despite the similar locations, variations were observed between the global orientations of these macrolide families and that their peculiar orientation, as well as the conformations of the lactone rings of the 16-membered macrolides, leads to only partial blockage of the tunnel (Figure 9) (29, 42).

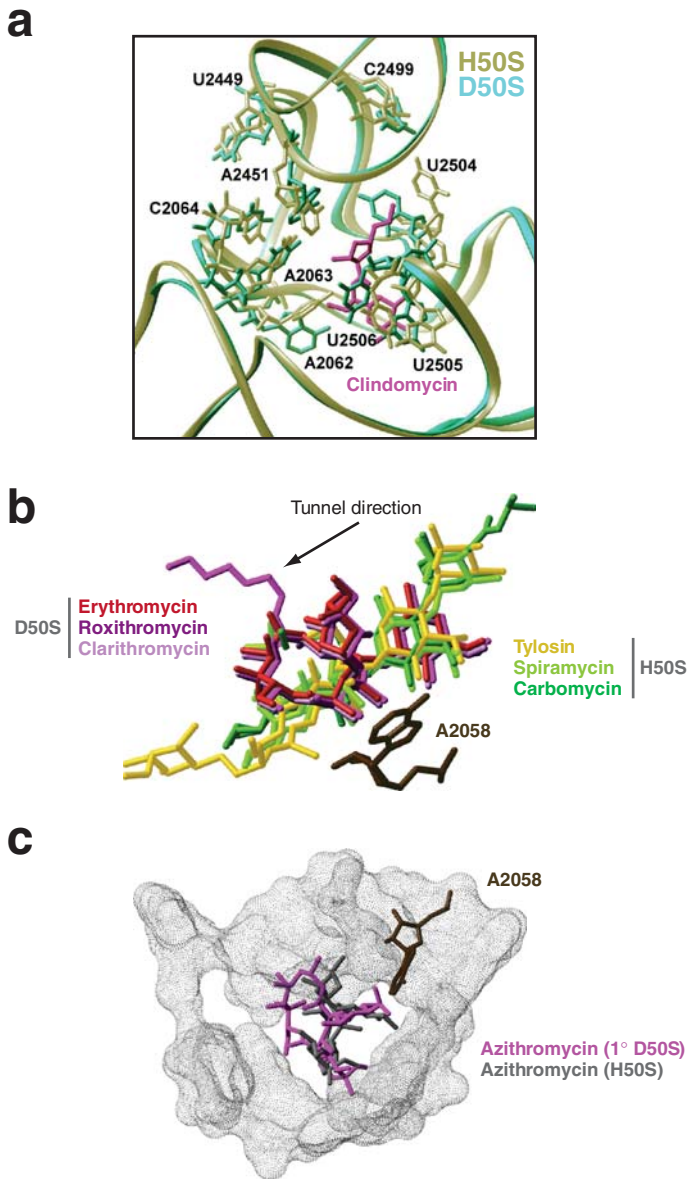
a
U2449
C2499
H50S
D50S
A2451
U2504
C2064
A2063
U2506
A2062
U2505
Clindomycin
b
Tunnel direction
D50S
Erythromycin
Roxithromycin
Clarithromycin
Tylosin
Spiramycin
Carbomycin
H50S
A2058
c
A2058
Azithromycin (1° D50S)
Azithromycin (H50S)

Selectivity Determined by Conformational and Sequence Variability

At the first glance, drug binding to ribosomes with guanine at position 2058 may indicate a low level of selectivity that should consequently reduce its clinical relevance. The wide usage of azithromycin indicates the contrary. This can be explained by comparing the azithromycin-binding modes to D50S and to H50S, assuming that H50S represents, to some extent, the eukaryotic ribosome. Thus, in H50S, azithromycin blocks only a relatively small part of the tunnel (19), whereas in D50S, the azithromycin molecule that occupies the high-affinity macrolide pocket (called Azi-1) should lead to effective blockage of the exit tunnel (Figure 9) (18, 29, 42). These prominent differences in binding modes suggest that additional factors influence drug interactions. Indeed, considerable differences in the fine structures of the environment of the macrolide-binding pocket have been identified by a careful comparison of drug binding modes to ribosomes of two kingdoms, eubacteria and archaea (42), explaining also the typical requirement for an immense excess of antibiotics for meaningful antibiotic binding to H50S.

The amount of antibiotics required for meaningful binding to ribosomes from different sources provides an additional distinction between antibiotic-binding modes. Thus, clinically meaningful binding of antibiotics to the small ribosomal subunits from *T. thermophilus*, T30S, and the large ribosomal subunit from *D. radiodurans*, D50S, could be achieved with an antibiotic concentration similar to those found effective for therapeutic use. In contrast, antibiotic binding to the large subunits from *H. marismortui*, H50S, necessitates up to 1000-fold excess of the commonly used concentrations in therapeutic treatment (19, 20). Hence, the crystallographically observed differences in the antibiotic-binding modes of these two forms demonstrate the interplay between structure and clinical implications

←

Figure 9 (*a*) Conformational differences between H50S and D50S nucleotides around the clindamycin-binding site. The subset of clindamycin interactions with the PTC is shown. Note the similarity of the RNA backbones, in contrast to the pronounced differences of the orientations of the bases. (*b*) Superposition of the locations of three 16-membered macrolides: tylosin, spiramycin and carbomycin bound to H50S, on the locations of the three 14-membered macrolides bound to D50S, as shown in Figure 7a. Note the larger distance between the nucleotide at position 2058 and the desosamine sugars of the three 16-membered macrolides, compared to the 14-member compounds. Also note that superiority in tunnel blocking effectiveness of the 14-membered macrolides over the 16-member compounds, as the latter seems to hardly hamper nascent protein passage. (*c*) A section of the exit tunnel (shown as a *gray cloud*) with the positions of azithromycin in H50S (AZI-H) and one of the two azithromycin molecules that bind to D50S (AZI_1-D). This figure shows that the binding mode of this azithromycin molecule to D50S is similar to that of typical macrolides to eubacterial pathogens and that this molecule alone should arrest nascent protein passage. For orientation, the position on A2059 is shown.

and illuminate the distinction between medically meaningful and less relevant binding.

In general, variations in binding modes of the same drugs to H50S and D50S can be correlated with conformational differences originating from phylogenetic differences between these two species (42); from the functional state of the crystallized material, as seen in the case of sparsomycin described above (29); and from the gap between physiologically active conditions and specific crystal environments. Examples of variability that do not depend on adenine/guanine exchange are chloramphenicol, clindamycin, and streptogramin$_A$.

In accord with chloramphenicol selectivity, even at exceptionally high chloramphenicol amounts, binding at the PTC A site was not detected in the H50S complex. Instead, another site was found at the entrance to the ribosomal tunnel (20) in a position that does not interfere with peptide-bond formation or with nascent chain progression; therefore, binding leads to marginal or to no inhibitory significance (29) as well as to apparent competition with macrolides. Lack of chloramphenicol binding to the A site in the PTC of H50S may be the consequence of the H50S crystal environment, which hardly resembles the in situ environment within either typical pathogens or the *H. marismortui* cell (11, 33), particularly the ratios between mono and divalent ions. Variations in ion types and concentrations were shown to induce significant conformational alterations in the PTC (96, 97) that may lead to inactivation and to reduction of the efficiency of A-site tRNA binding (98) as well as the affinity for chloramphenicol.

Yet another cause for lack of chloramphenicol binding to the PTC of H50S may be associated with the *H. marismortui* PTC conformation, which was found to differ from that of PTC in the eubacterial ribosome (12) and also differs in the unbound eubacterial large subunit (Figure 9) (13, 33). Assuming that the PTC of H50S resembles that of eukaryotes, the significant differences between its conformation and that of eubacteria seems to be the reason for the rather low affinity of PTC antibiotics to eukaryotes. The lack of clindamycin binding to H50S is an additional example that can be explained by inherent conformational difference between eubacteria and eukaryotes. Thus, almost all interactions of this drug with the PTC of the eubacterial D50S cannot be formed by the corresponding H50S moieties, because they point in directions that are not suitable for interactions.

Streptogramin presents an interesting case of double selectivity. As shown above, upon binding to D50S dalfopristin, the streptogramin$_A$-like component of Synercid®, nucleotide U2585, undergoes a remarkable flip of almost 180° rotation. In contrast, in the complex of H50S with a streptogramin$_A$-like component, called Virginiamycin-M, the U2585 conformation is hardly altered (20). This mild drug action is explained by the different conformations of the PTC of H50S compared to those of the eubacterial ribosomes (12, 13), in accord with the inability of chloramphenicol (20), a known A-site competitor (43–45), to bind to the PTC of H50S. The streptogramin$_B$ component of Synercid® is a modified macrolide, which binds to the macrolide high-affinity pocket through A2058. Consistently, no streptogramin$_B$ binding to H50S was detected (20), presumably because the archaeon *H. marismortui* possesses a guanine in position 2058. The apparent

contradiction between the lack of streptogramin$_B$ binding to crystalline H50S and the genetic experiments indicating that streptogramin$_B$ binds to *H. halobium* (92) can be explained by weak binding, which is at a level insufficient for crystallographic detection, by the further distance of *H. marismortui* from eubacteria (compared to *H. halobium*), or by additional conformational changes induced far from the physiological crystal environment (11). Indeed, lack of streptogramin$_B$ interactions with H50S is not surprising because on the basis of D50S structures complexed with various macrolides such binding requires adenine in position 2058.

INDIRECT AND ALLOSTERIC EFFECTS

Structural investigations on genuine pathogens are restricted for a variety of reasons, including the difficulties in crystallization of their ribosomes. Therefore, the current knowledge of the molecular detail of antibiotic interactions with ribosomes emerged from the only species that yielded well-diffracting crystals of ribosomal particles. Two of those are eubacteria (*T. thermophilus* and *D. radiodurans*), resembling *E. coli*, a eubacterium that may become pathogenic (99) and its ribosome were intensively investigated, and the third is an archaeon, namely *H. marismortui.* The latter possesses partial sequence identity with eukaryotes, and its ribosomal crystals contain high salinity (~2M NaCl) (11), thus further limiting its usefulness as a model.

Similar considerations apply to the shortcomings of biochemical and genetic studies because many bacteria possess multiple genes, which may lead to ambiguous results. In addition, phylogenetic differences between various bacteria imply that even the usage of specific pathogens may not provide information that could be extended to all pathogens because each pathogen represents only itself. The main criteria for selecting or designing suitable models predominantly concern the possibility of producing antibiotic-ribosome complexes in close to clinically relevant concentrations. Minimizing the deviations from the in situ pathogenic cell environment is also important. Furthermore, species with a single rRNA operon chromosomal copy, such as *H. halobium* (43), are beneficial for mutagenesis-based studies, although occasionally they have led to misinterpretations (100). Genetically engineered pathogen models, such as *Mycobacterium smegmatis* (101), should be advantageous for the description of genuine pathogens, as they can provide isogenic mutations (30).

For decades most of the biochemical and genetic studies were performed on *E. coli* ribosome. The choice of *E. coli* as a pathogen representative, despite its inherent instability and complex genome, may be justified in view of findings that it binds antibiotics in a fashion similar to many pathogens. The usage of *E. coli* yielded valuable information alongside questionable conclusions, such as the existence of direct interactions between macrolides and domain II RNA (70, 71). *E. coli* is also the organism that revealed mutations in proteins L4 and L22, which rendered resistance to erythromycin (102, 103); this was reconfirmed later in several pathogens, such as macrolide-susceptible *Streptococcus pneumoniae*

(104). Although direct interactions were not detected between erythromycin and these proteins in D50S (17), cryo EM studies (105) on ribosomes with mutated protein L22 revealed a possible conformational change in the tunnel diameter, consistent with results of the superposition of the crystal structure of the L22 deletion mutant (106) on that of D50S. Furthermore, the suggestion that perturbing the tunnel conformation can trigger additional conformational alterations (107) could be correlated with the inherent flexibility of L22 beta-hairpin (21).

It has been shown that the tip of L22 beta-hairpin swings across the tunnel upon troleandomycin binding (21), in a fashion suggesting that a similar motion is involved in tunnel gating. The interactions of the drug with either sides of the tunnel side support this suggestion because it seems that the conformations of both sides are designed for this purpose (21, 32). Further analysis of the region interacting with L22 at its swung conformation revealed a possible interaction between the L22 beta-hairpin tip and protein L4. Thus, only minute conformational rearrangements were needed in order to create a "nest," accommodating a protein L4 loop (Figure 7), which indicates a possible cross correlation between these two proteins.

Similarly, no interactions between tiamulin and protein L3 have been detected crystallographically. Nevertheless, L3 tiamulin-resistant mutations are known, and these are usually accompanied by an additional 23S rRNA mutation (54). Another example is the alteration in U2584 accessibility (53) upon tiamulin binding, although no direct interactions of tiamulin with U2584 were observed. In this case, a plausible explanation can be given because tiamulin binding to U2506, U2585, and G2586 reduces the space between U2584 and the tunnel wall.

Mutations in proteins L22 and L4 that cause resistance to telithromycin in ribosomes with A2058G mutation or methylation were detected in several pathogens (108,109) as well as in a genetically engineered pathogen model (E. Boettger and N. Corti, private communication). In its complex with D50S, the position of telithromycin allows interactions with Arg 90 of L22 through its carbamate ring (R. Berisio, private communication). However, the difference electron density map in this region does not indicate a stable interaction because it is rather fragmented and because the Arg 90 side chain is poorly resolved, suggesting that its conformation is not fixed by any contacts. A similar feature, namely fragmented electron density in the vicinity of the swung conformation of the L22 beta-hairpin tip, was also identified in electron density maps of D50S complexes with other compounds, such as laboratory derivatives of various macrolides (not necessarily the 15- or 16-member lactone ring).

The interactions between protein L22 and large macrolides or ketolides, such as telithromycin, may intensify upon G mutation or *erm* methylation of A2058 because it is likely that the additional space consumed by the mutated or methylated 2058 will "push" the macrolide away, so a new set of interactions can be formed deeper in the tunnel (R. Berisio, private communication). Moreover, by losing the tight 2058-desosamine interactions, telithromycin may gain a higher level of conformational freedom. Owing to its size, telithromycin, as well as other large macrolides or ketolides, can reach other regions of the tunnel and utilize additional

interactions compensating for the lost of the traditional 2058 contacts. In this way, potential telithromycin interactions with L22 may gain weight in efficient antibiotic binding. Hence, mutations or deletions in the L22 beta-hairpin tip can induce resistance. Importantly, the region of L22 mutated in telithromycin resistant strains corresponds to the L22 region that swings upon troleandomycin binding (E. Boettger and N. Corti, private communication).

FUTURE PROSPECTS

Numerous attempts at combating pathogen resistance are being made by endeavors to improve existing antibiotics and by the design of novel compounds. The results of these efforts indicate clearly that the battle is far from its end and that additional major effort is necessary. The crystallographic structures of the antibiotic complexes with the bacterial ribosome alongside the identification and/or engineering of suitable pathogen models should provide insights for this goal.

High-resolution structures show that the combination of the binding pocket environment with the antibiotic's chemical properties governs its in situ conformation and the nature of its interactions with the ribosome. Hence, similar, or even indistinguishable, modes of action do not necessarily imply the same binding modes. Furthermore, variations in drug properties appear to govern the exact nature of seemingly identical mechanisms of drug resistance. For these reasons, the observed variability in binding modes justifies expectations for the design of improved antibiotic properties by chemical modifications of existing compounds as well as by the design of novel drugs, using structural information.

Also gratifying are recent reports on utilizing the structural information for therapeutic usage of antibiotics for additional treatments, which are not based on the anti-infective action of the antibiotics. An example is the use of the aminoglycoside antibiotic gentamicin in the management of severe deficiency in chloride-channel activity in cystic fibrosis patients (110). Because gentamicin facilitates bypass of termination codons, it allows the expression of full-length protein in individuals who have a premature termination signal in their cystic fibrosis transmembrane conductance regulator gene.

CONCLUSIONS

Continuous research on ribosomal antibiotics, enriched by recent three-dimensional structural information, showed that, despite the significant diversity in antibiotic modes of action, several common traits exist.

- Although theoretically the giant ribosome offers numerous binding opportunities, ribosomal antibiotics bind to a single or a few binding sites.
- Most antibiotics interact primarily with ribosomal RNA and cause minor conformational changes.

- Minute structural differences, scattered in various ribosomal locations, are responsible for antibiotic selectivity and efficiency.
- The characteristics of antibiotic-binding modes are dictated by parameters such as the species-specific composition of its binding pocket and its conformation, the functional state of the ribosome, and the exact chemical nature of the drug.
- Resistance to ribosomal antibiotics is acquired mainly by alterations in the target.
- In a few cases, the antibiotic chemical moieties are modified.
- The primary action of most antibiotics that induce significant local or allosteric conformational alterations is to inhibit functional activities.
- Most proteins that interact with antibiotics are involved in dynamic aspects of ribosomal function.

Although a precise understanding of all processes associated with antibiotic action is incomplete, the current findings justify modest optimism. Thus, it appears that the elucidation of some common principles, combined with the genetic, structural, and biochemical knowledge, should lead to structure-based approaches to be used in devising modifications of existing antibiotics as well as in the design of novel potent anti-infective drugs.

ACKNOWLEDGMENTS

Thanks are due to Dr. I. Shalit and to all members of the ribosome group at the Weizmann Institute, Israel, and to all members of the former Max Planck Research Unit in Hamburg. Drs. A. Bashan and M. Kessler provided excellent assistance in the preparation of this review. X-ray diffraction data were collected at ID19/SBC/APS/ANL and ID14/ESRF-EMBL. The U.S. National Institutes of Health (GM34360), the Human Frontier Science Program Organization (HFSP: RGP0076/2003), the Kimmelman Center for Macromolecular Assemblies, and Pfizer Global Research & Development provided support. AY holds the Martin and Helen Kimmel Professorial Chair.

The *Annual Review of Biochemistry* is online at http://biochem.annualreviews.org

LITERATURE CITED

1. Sigmund CD, Ettayebi M, Morgan EA. 1984. *Nucleic Acids Res.* 12:4653–63
2. Courvalin P, Ounissi H, Arthur M. 1985. *J. Antimicrob. Chemother.* 16:91–100
3. Weisblum B. 1995. *Antimicrob. Agents Chemother.* 39:577–85
4. Vazquez D. 1979. *Mol. Biol. Biochem. Biophys.* 30:1–312
5. Cundliffe E, 1981. In *The Molecular Basis of Antibiotic Action*, ed. EF Gale, E Cundliffe, PE Reynolds, MH Richmond, MJ Waring MJ, pp. 419–39. London: Wiley

6. Cundliffe E. 1981. See Ref. 5, pp. 402–547
7. Spahn CM, Prescott CD. 1996. *J. Mol. Med.* 74:423–39
8. Yonath A, Bashan A. 2004. *Annu. Rev. Microbiol.* 58:233–51
9. Schluenzen F, Tocilj A, Zarivach R, Harms J, Gluehmann M, et al. 2000. *Cell* 102:615–23
10. Wimberly BT, Brodersen DE, Clemons WM Jr, Morgan-Warren RJ, Carter AP, et al. 2000. *Nature* 407:327–39
11. Ban N, Nissen P, Hansen J, Moore PB, Steitz TA. 2000. *Science* 289:905–20
12. Yusupov MM, Yusupova GZ, Baucom A, Lieberman K, Earnest TN, et al. 2001. *Science* 292:883–96
13. Harms J, Schluenzen F, Zarivach R, Bashan A, Gat S, et al. 2001. *Cell* 107: 679–88
14. Carter AP, Clemons WM, Brodersen DE, Morgan-Warren RJ, Wimberly BT, Ramakrishnan V. 2000. *Nature* 407:340–48
15. Brodersen DE, Clemons WM Jr, Carter AP, Morgan-Warren RJ, Wimberly BT, Ramakrishnan V. 2000. *Cell* 103:1143–54
16. Pioletti M, Schluenzen F, Harms J, Zarivach R, Gluehmann M, et al. 2001. *EMBO J.* 20:1829–39
17. Schluenzen F, Zarivach R, Harms J, Bashan A, Tocilj A, et al. 2001. *Nature* 413:814–21
18. Schluenzen F, Harms JM, Franceschi F, Hansen HA, Bartels H, et al. 2003. *Structure* 11:329–38
19. Hansen JL, Ippolito JA, Ban N, Nissen P, Moore PB, Steitz TA. 2002. *Mol. Cell* 10:117–28
20. Hansen JL, Moore PB, Steitz TA. 2003. *J. Mol. Biol.* 330:1061–75
21. Berisio R, Schluenzen F, Harms J, Bashan A, Auerbach T, et al. 2003. *Nat. Struct. Biol.* 10:366–70
22. Berisio R, Harms J, Schluenzen F, Zarivach R, Hansen HA, et al. 2003. *J. Bacteriol.* 185:4276–79
23. Harms J, Schluenzen F, Fucini P, Bartels H, Yonath A. 2004. *BMC Biol.* 2:1741–47
24. Schluenzen F, Pyetan E, Yonath A, Harms J. 2004. *Mol. Microbiol.* 54:1287–94
25. Auerbach T, Bashan A, Harms J, Schluenzen F, Zarivach R, et al. 2002. *Curr. Drug Targets—Infect. Disord.* 2:169–86
26. Knowles DJ, Foloppe N, Matassova NB, Murchie AI. 2002. *Curr. Opin. Pharmacol.* 2:501–6
27. Gaynor M, Mankin AS. 2003. *Curr. Top Med. Chem.* 3:949–61
28. Poehlsgaard J, Douthwaite S. 2003. *Curr. Opin. Investig. Drugs* 4:140–48
29. Auerbach T, Bashan A, Yonath A. 2004. *Trends Biotechnol.* 22:570–76
30. Pfister P, Jenni S, Poehlsgaard J, Thomas A, Douthwaite S, et al. 2004. *J. Mol. Biol.* 342:1569–81
31. Bashan A, Agmon I, Zarivach R, Schluenzen F, Harms J, et al. 2003. *Mol. Cell* 11: 91–102
32. Agmon I, Amit M, Auerbach T, Bashan A, Baram D, et al. 2004. *FEBS Lett.* 567:20–26
33. Yonath A. 2002. *Annu. Rev. Biophys. Biomol. Struct.* 31:257–73
34. Lodmell JS, Dahlberg AE. 1997. *Science* 277:1262–67
35. Fourmy D, Recht MI, Blanchard SC, Puglisi JD. 1996. *Science* 274:1367–71
36. Vicens Q, Westhof E. 2001. *Structure* 9:647–58
37. Lynch SR, Gonzalez RL, Puglisi JD. 2003. *Structure* 11:43–53
38. Fourmy D, Recht MI, Puglisi JD. 1998. *J. Mol. Biol.* 277:347–62
39. Bashan A, Zarivach R, Schluenzen F, Agmon I, Harms J, et al. 2003. *Biopolymers* 70:19–41
40. Agmon I, Auerbach T, Baram D, Bartels H, Bashan A, et al. 2003. *Eur. J. Biochem.* 270:2543–56
41. Zarivach R, Bashan A, Berisio R, Harms J, Auerbach T, et al. 2004. *J. Phys. Org. Chem.* 17:901–12
42. Baram D, Yonath A. 2005. *FEBS Letters.* 579:948–54

43. Mankin AS, Garrett RA. 1991. *J. Bacteriol.* 173:3559–63
44. Shaw WV, Leslie AG. 1991. *Annu. Rev. Biophys. Biophys. Chem.* 20:363–86
45. Izard T, Ellis J. 2000. *EMBO J.* 19:2690–700
46. Douthwaite S. 1992. *Nucleic Acids Res.* 20:4717–20
47. Kucers A, Bennett N, Kemp R. 1987. In *The Use of Antibiotics*, ed. A Kucers, N Bennett, R Kemp, pp. 819–50. Philadelphia: Heinemann
48. Bacque E, Pautrat F, Zard SZ. 2002. *Chem. Commun.* 2312–13
49. Springer DM, Sorenson ME, Huang S, Connolly TP, Bronson JJ, et al. 2003. *Bioorg. Med. Chem. Lett.* 13:1751–53
50. Kavanagh F, Hervey A, Robbins WJ. 1951. *Proc. Natl. Acad. Sci. USA* 37:570–74
51. Egger H, Reinshagen H. 1976. *J. Antibiot.* 29:923–27
52. Hogenauer G. 1975. *Eur. J. Biochem.* 52: 93–98
53. Poulsen SM, Karlsson M, Johansson LB, Vester B. 2001. *Mol. Microbiol.* 41:1091–99
54. Pringle M, Poehlsgaard J, Vester B, Long KS. 2004. *Mol. Microbiol.* 54:1295–306
55. Hogenauer G, Egger H, Ruf C, Stumper B. 1981. *Biochemistry* 20:546–52
56. Milligan RA, Unwin PN. 1986. *Nature* 319:693–95
57. Yonath A, Leonard KR, Wittmann HG. 1987. *Science* 236:813–16
58. Nissen P, Hansen J, Ban N, Moore PB, Steitz TA. 2000. *Science* 289:920–30
59. Nakatogawa H, Ito K. 2002. *Cell* 108: 629–36
60. Gong F, Yanofsky C. 2002. *Science* 297:1864–67
61. Woolhead CA, McCormick PJ, Johnson AE. 2004. *Cell* 116:725–36
62. Andersson S, Kurland CG. 1987. *Biochimie* 69:901–4
63. Contreras A, Vazquez D. 1977. *Eur. J. Biochem.* 74:539–47
64. Tai PC, Wallace BJ, Davis BD. 1974. *Biochemistry* 13:4653–59
65. Tenson T, Lovmar M, Ehrenberg M. 2003. *J. Mol. Biol.* 330:1005–14
66. Garza-Ramos G, Xiong L, Zhong P, Mankin A. 2001. *J. Bacteriol.* 183:6898–907
67. Tenson T, Ehrenberg M. 2002. *Cell* 108: 591–94
68. Menninger JR, Otto DP. 1982. *Antimicrob. Agents Chemother.* 21:811–18
69. Otaka T, Kaji A. 1975. *Proc. Natl. Acad. Sci. USA* 72:2649–52
70. Douthwaite S, Hansen LH, Mauvais P. 2000. *Mol. Microbiol.* 36:183–93
71. Vester B, Douthwaite S. 2001. *Antimicrob. Agents Chemother.* 45:1–12
72. Blondeau JM, DeCarolis E, Metzler KL, Hansen GT. 2002. *Expert Opin. Investig. Drugs* 11:189–215
73. Le Noc P, Croize J, Bryskier A, Le Noc D, Robert J. 1989. *Pathol. Biol.* 37:553–59
74. Bryskier A, Butzler JP, Neu HC, Tulkens PM, eds. 1993. *Macrolides-Chemistry, Pharmacology, and Clinical Uses*. Paris: Blackwell
75. Poulsen SM, Kofoed C, Vester B. 2000. *J. Mol. Biol.* 304:471–81
76. Alvarez-Elcoro S, Enzler MJ. 1999. *Mayo Clin. Proc.* 74:613–34
77. Champney WS, Tober CL. 2000. *Curr. Microbiol.* 41:126–35
78. Bryskier A. 2001. *Jpn. J. Antibiot.* 54:64–69
79. Zhong P, Shortridge V. 2001. *Curr. Drug Targets Infect. Disord.* 1:125–31
80. Wu YJ, Su WG. 2001. *Curr. Med. Chem.* 8:1727–58
81. Zhanel GG, Walters M, Noreddin A, Vercaigne LM, Wierzbowski A, et al. 2002. *Drugs* 62:1771–804
82. Ackermann G, Rodloff AC. 2003. *J. Antimicrob. Chemother.* 51:497–511
83. Douthwaite S, Champney WS. 2001. *J. Antimicrob. Chemother.* 48:1–8
84. Xiong L, Shah S, Mauvais P, Mankin AS. 1999. *Mol. Microbiol.* 31:633–39

85. Hansen LH, Mauvais P, Douthwaite S. 1999. *Mol. Microbiol.* 31:623–31
86. Bingen E, Leclercq R, Fitoussi F, Brahimi N, Malbruny B, et al. 2002. *Antimicrob. Agents Chemother.* 46:1199–203
87. Vimberg V, Xiong L, Bailey M, Tenson T, Mankin A. 2004. *Mol. Microbiol.* 54:376–85
88. Tenson T, DeBlasio A, Mankin A. 1996. *Proc. Natl. Acad. Sci. USA* 93:5641–46
89. Tenson T, Mankin AS. 2001. *Peptides* 22:1661–68
90. Tripathi S, Kloss PS, Mankin AS. 1998. *J. Biol. Chem.* 273:20073–77
91. Mao JC, Robishaw EE. 1971. *Biochemistry* 10:2054–61
92. Porse BT, Garrett RA. 1999. *J. Mol. Biol.* 286:375–87
93. Porse BT, Kirillov SV, Awayez MJ, Ottenheijm HC, Garrett RA. 1999. *Proc. Natl. Acad. Sci. USA* 96:9003–8
94. Goldberg IH, Mitsugi K. 1966. *Biochem. Biophys. Res. Commun.* 23:453–59
95. Monro RE, Celma ML, Vazquez D. 1969. *Nature* 222:356–58
96. Zamir A, Miskin R, Vogel Z, Elson D. 1974. *Methods Enzymol.* 30:406–26
97. Bayfield MA, Dahlberg AE, Schulmeister U, Dorner S, Barta A. 2001. *Proc. Natl. Acad. Sci. USA* 98:10096–101
98. Moore PB, Steitz TA. 2003. *RNA* 9:155–59
99. Kaper JB, Nataro JP, Mobley HL. 2004. *Nat. Rev. Microbiol.* 2:123–40
100. Tan GT, DeBlasio A, Mankin AS. 1996. *J. Mol. Biol.* 261:222–30
101. Boettger EC, Springer B, Prammananan T, Kidan Y, Sander P. 2001. *EMBO Rep.* 2:318–23
102. Wittmann HG, Stoffler G, Apirion D, Rosen L, Tanaka K, et al. 1973. *Mol. Gen. Genet.* 127:175–89
103. Chittum HS, Champney WS. 1994. *J. Bacteriol.* 176:6192–98
104. Canu A, Abbas A, Malbruny B, Sichel F, Leclercq R. 2004. *Antimicrob. Agents Chemother.* 48:297–304
105. Gabashvili IS, Gregory ST, Valle M, Grassucci R, Worbs M, et al. 2001. *Mol. Cell* 8: 181–88
106. Davydova N, Streltsov V, Wilce M, Liljas A, Garber M. 2002. *J. Mol. Biol.* 322:635–44
107. Gregory ST, Dahlberg AE. 1999. *J. Mol. Biol.* 289:827–34
108. Bozdogan B, Appelbaum PC, Kelly LM, Hoellman DB, Tambic-Andrasevic A, et al. 2003. *Clin. Microbiol. Infect.* 9:741–45
109. Pereyre S, Gonzalez P, De Barbeyrac B, Darnige A, Renaudin H, et al. 2002. *Antimicrob. Agents Chemother.* 46:3142–50
110. Wilschanski M, Yahav Y, Yaacov Y, Blau H, Bentur L, et al. 2003. *N. Engl. J. Med.* 349:1433–41